Lattice Boltzmann method for fluid flow around bodies using volume penalization

M. Benamour*, E. Liberge and C. Béghein
LaSIE, UMR CNRS 7356, University of La Rochelle, Avenue Michel Crépeau, 17042, La Rochelle Cedex, France

ABSTRACT
This paper deals with the implementation of a volume penalization technique in a lattice Boltzmann model, in order to compute flows around obstacles. The penalization term was introduced into the lattice Boltzmann equation via a forcing term. This approach was applied to the one dimensional Burgers equation for motionless and moving obstacles (forced motion, and coupling between the fluid force calculated with the penalized Burgers equation and the motion of the obstacle), and to the two dimensional Navier-Stokes equation, for motionless obstacles (flows over a square obstacle, and past a circular cylinder). A good agreement with numerical results obtained with other techniques, and with results found in literature was obtained.

Keywords: Penalization technique, Lattice Boltzmann, CFD, Fluid Structure Interaction (FSI)

1. INTRODUCTION

Flows around moving obstacles are encountered in many applications such as particle laden flows, flows around ships, sailing boats, wind turbines, aircrafts, and so on. Due to the increasing performance of computers, numerical simulation becomes an attractive tool for predicting such flows. The lattice Boltzmann method (LBM), which is easy to implement, involves local computations, and is thus well suited for parallel computing, is a good candidate for solving the equations that describe flows around moving objects. Various techniques have been developed in the past to model particles moving in fluids, in the lattice Boltzmann framework.

In his pioneering work, Ladd [1, 2], used the bounce back rule to model the no-slip boundary condition between the particle and fluid, and developed the momentum exchange method to calculate the fluid force exerted on the solid particle.

Noble and Torczynski [3], proposed to modify the collision term in the lattice Boltzmann equation, to account for the interaction between a solid obstacle and the lattice nodes. With this method, the conventional lattice Boltzmann equation was recovered for fluid regions without obstacle, and rigid body motion (i.e. the Zou and He bounce back rule [4]) was obtained in regions occupied only by the solid obstacle. This method was applied successfully to the computation of flow around a periodic line of oscillatory moving cylinders.

The immersed boundary method, which was introduced in the 1970s by Peskin [5] to model blood flow in the heart, and which employs a fixed cartesian mesh for the fluid and

*Corresponding Author: E-mail: malek.benamour@univ-lr.fr

lagrangian nodes attached to the moving boundary, and adds a forcing term in the Navier-Stokes equations to model the influence of the boundary on the fluid flow, was adapted to the LBM for flows around rigid particles by Feng and Michaelides [6], and by Ten Cate et al. [7]. The forcing term was modeled by Feng and Michaelides with a restauration force acting on the particle boundary. Ten Cate et al. used for this term a variant developed by Goldstein et al. [8], where the restauration force on the boundary can be due, from a physical point of view, to a damped oscillator. The drawback of this method was that results depended on one or two empirical parameters. To avoid this problem, Feng and Michaelides [9], and Dupuis et al. [10], introduced into the IB-LBM (Immersed Boundary – lattice Boltzmann method), the direct forcing approach proposed by Fadlun et al. [11]. In this approach, the forcing point was located in the fluid region in the immediate vicinity of the solid boundary, and an interpolation between the solid points and the fluid points was used to evaluate the forcing term. With this approach, the no-slip conditon is not exactly satisfied at the solid boundary, and some streamlines may penetrate in the solid obstacle. To enforce the no-slip condition at the solid boundary, Wu and Shu [12], by using the formulation of the forcing term proposed by Guo et al. [13], developed an implicit procedure, where a velocity correction was calculated for all lagrangian points at the boundary. Owing to the fact that the fluid domain is not remeshed when applying the immersed boundary method, this technique is now frequently used in the lattice Boltzmann method. However, other approaches have been implemented in the lattice Boltzmann framework.

Among these, we can cite the Distributed Lagrange Multiplier/Fictitious Domain approach (DLM/FD) [14]. Shi and Phan-Thien [15] applied to the lattice Boltzmann method the DLM/FD formulation developed by Yu [16]. In this approach, the fluid equation was solved on a fictitious domain including the fluid domain and the solid domain, and a force (the Lagrange multiplier) was introduced to force the velocity of the fictitious fluid inside the solid domain to be the same as the solid velocity. The solid domain was followed with a Lagrangian description. With this method, the remeshing procedure, which is computationally time consuming, was avoided.

Very recently, Meldi et al. [17] applied the Arbitrary Lagrangian Eulerian formulation to the LBM. In the Arbitrary Lagrangian Eulerian description, the grid is divided into two parts: a fixed one, and a moving one which follows for example the flow around a moving obstacle. The nodes of the moving grid are displaced arbitrarily using a Lagrangian description. In this region, the Navier-Stokes equations are solved on the moving grid [18]. Using the Chapman-Enskog procedure, Meldi et al. developed the lattice Boltzmann formulation for a moving grid. Non-deforming grids were chosen. They applied this technique successfully to the computation of flows around non-deforming obstacles.

In this work, we wish to implement the volume penalization technique, to compute flows around obstacles, with the lattice Boltzmann method. The volume penalization technique consists in introducing a volume penalization term into the equation that needs to be solved, in order to take into account the influence of the obstacle on the fluid domain [19, 20]. Since this equation is solved on both fluid and solid domains, the boundary conditions at the fluid-solid interface are naturally applied. Hence this method appears to be easy to implement, and to parallelize in a lattice Boltzmann framework. In this paper, we applied, in a first step, the volume penalization technique to the one dimensional Burgers equation, which was solved with the lattice Boltzmann method. Several cases were investigated: non moving obstacle, imposed motion of the obstacle, coupling between Burgers equation and the motion of the obstacle. In a second step, the volume penalization approach was implemented in the Navier-Stokes equations, which were solved with the lattice Boltzmann method. Two cases were

considered: flow past a square obstacle, and flow past a circular obstacle. In the last section of the paper, conclusions and future work are pointed out.

2. ONE DIMENSIONAL BURGERS EQUATION

Let us consider a domain Ω, composed of a fluid domain $\Omega_f(t)$ (wheren t denotes time), and a solid domain $\Omega_s(t)$, where the fluid solid interface $X_s(t)$ may move according to time (see Figure 1).

The volume penalization technique was applied in this paragraph to the one dimensional Burgers equation. The one dimensional Burgers equation, with a volume penalization term, reads:

$$\frac{\partial(u)}{\partial t}+\frac{\partial}{\partial x}\left(\frac{u^2}{2}\right)=\frac{\partial}{\partial x}\left(\nu\frac{\partial u}{\partial x}\right)-\frac{1}{\eta}\left(\chi\left(u-u_s\right)\right) \tag{1}$$

Where u is the velocity according to x direction, ν is the kinematic viscosity of the fluid. In the penalization term, χ is a mask function, which is equal to 0 in the fluid domain $\Omega_f(t)$, and to 1 in the solid domain $\Omega_s(t)$, η is a permeability coefficient that is very high in the fluid domain and very small in the solid domain, and u_s is the obstacle velocity. In the fluid domain, the ratio χ/η is null, hence the penalization term vanishes. In the solid domain, the ratio χ/η is very high, the velocity is thus equal to the solid velocity.

In order to solve this equation with the lattice Boltzmann method, the lattice Boltzmann model for a non linear convection diffusion equation developed by Shi and Guo [21] was selected. The lattice Boltzmann equation, with the single relaxation time Bhatnagar-Gross-Krook (BGK) collision operator, is:

$$f_\alpha\left(\vec{x}+\vec{e}_\alpha\Delta t, t+\Delta t\right)=f_\alpha\left(\vec{x}, t\right)-\frac{1}{\tau}\left(f_\alpha\left(\vec{x}, t\right)-f_\alpha^{eq}\left(\vec{x}, t\right)\right)+\Delta t F_\alpha \tag{2}$$

Where $f_\alpha\left(\vec{x}, t\right)$ is the probability of finding a fluid particle with velocity $\vec{e}_\alpha$ at position $\vec{x}$ and time t, Δt is the time step, τ is the non dimensional relaxation time, f_α^{eq} is the equilibrium distribution function, F_α is the forcing term that takes into account, in our study, the penalization term. For this one dimensional case, the $D1Q3$ model was used. In this model, the lattice velocities are $\{\vec{e}_0, \vec{e}_1, \vec{e}_2\}=\{0, c, -c\}$, where $c = \Delta x/\Delta t$, and x is the lattice spacing, the values of the weight coefficients are ω_0 = 2/3, ω_1 = ω_2 = 1/6, the sound speed is $c_s = c/\sqrt{3}$. Shi and Guo showed that the equilibrium distribution function is:

$$f_\alpha^{eq}\left(\vec{x}, t\right)=\omega_\alpha\left[u+\frac{\vec{e}_\alpha.\,\vec{B}}{c_s^2}+\frac{\left(C-c_s^2uI\right):\left(\vec{e}_\alpha\,\vec{e}_\alpha-c_s^2I\right)}{2c_s^4}\right] \tag{3}$$

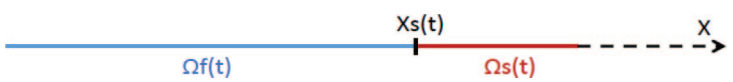

Figure 1: Configuration studied

Where $\vec{B}$ is the convective term in the macroscopic equation (in the case modeled here: $\vec{B} = \frac{u^2}{2}\vec{x}_0, \vec{x}_0$ is the unit vector according to direction), $C = C_0(u) + c_s^2 DI$, with $[C_0(u)]_{\alpha\beta} = \int B'_\alpha(u) B'_\beta(u)\,\mathrm{du}$, and $\vec{B}' = \frac{d\vec{B}}{du}$, D is the diffusive term in the macroscopic equation (in the case considered here: $D = u$), I is the identity tensor. The macroscopic variable is calculated with:

$$u = \sum_\alpha f_\alpha = \sum_\alpha f_\alpha^{eq} \tag{4}$$

and the relationship between the diffusion coefficient in Burgers equation, and the non dimensional relaxation time is: $\nu = c_s^2\left(\tau - \frac{1}{2}\right)\Delta t$. Shi and Guo obtained the following expression for the forcing term:

$$F_\alpha = \omega_\alpha F\left[1 + \lambda\frac{\vec{e}_\alpha \cdot \vec{B}'}{c_s^2}\right] \tag{5}$$

With the Chapman-Enskog analysis, they showed that λ is obtained from: $\lambda = \frac{\tau - 1/2}{\tau}$. When applying the penalization technique, instability occurs if the penalization term is treated explicitly. To circumvent this difficulty, an implicit treatment of the penalization term was adopted here. Using the Chapman-Enskog procedure, this led to the following expression for λ in the forcing term: $= \frac{\tau - 1/2}{\tau - 1}$. To test the suitability of the volume penalization technique to handle a moving obstacle with the lattice Boltzmann approach, the one dimensional Burgers equation was solved for three cases: non moving obstacle, imposed motion of the obstacle, coupling between Burgers equation and the motion of the obstacle. For each case, the LBM solution written in dimensional units was compared with a dimensional solution (an analytical solution or a numerical solution computed with the finite difference method).

2.1. MOTIONLESS OBSTACLE

Equation 1 was solved on the one dimensional domain $\Omega = [0; 1.2]$, where the fluid domain was $\Omega_f = [0; 1]$, and the solid domain was $\Omega_s = [1; 1.2]$. For this case, the solid domain did not move: $u(x, t) = u_s = 0, x \in \Omega_s$. The boundary condition on the left side of the fluid domain was: $u(0, t) = 0$. The initial condition was: $u(x, 0) = sin(\pi x), x \in \Omega_f$, and $u(x, 0) = 0, x \in \Omega_s$. For this case, we compared the exact solution in the fluid domain:

$$u(x,t) = 2\pi\nu\frac{\sum_{n=1}^{\infty} b_n \exp\left(-n^2\pi^2\nu t\right) n\,\sin\left(n\pi x\right)}{b_0 + \sum_{n=1}^{\infty} b_n \exp\left(-n^2\pi^2\nu t\right)\,cos\left(n\pi x\right)} \tag{6}$$

Where:

$$b_0 = \int_0^1 \exp\left(-(2\pi\nu)^{-1}\left[1-cos(\pi x)\right]\right) dx, \text{ and}$$

$$b_n = \int_0^1 \exp\left(-(2\pi\nu)^{-1}\left[1-cos(\pi x)\right]\right) cos(n\pi x)\, dx$$

with the numerical solution computed with the penalized Burgers equation and the lattice Boltzmann method. Figure 2 shows the exact solution, and the numerical one, at different times, for $\nu = 0.05\ m^2/s$, $\Delta x = 0.003333$ m (i.e. 301 lattice nodes), and $\Delta t = 1.85 \times 10^{-5} s$. The penalization coefficient was $\eta = 10^{-9}$. A satisfactory agreement can be noticed.

2.2. FORCED MOTION OF THE OBSTACLE

For this case, equation 1 was solved on the one dimensional domain $\Omega = [0; 1.2]$. The fluid-solid interface, of abscissa $x_s(t)$, moved with respect to time according to a linear law: $x_s(t) = At + B$, which led to a solid velocity: $x_s = A$. The initial condition was the same as in the previous case: $u(x, 0) = sin(\pi x)$, $x \in \Omega_f(0) = [0; 1]$, and : $u(x, 0) = 0, x \in \Omega_s(0) = [1; 1.2]$. The boundary condition on the left side of the fluid domain was: $u(0, t) = 0$. The fluid viscosity was: $\nu = 0.05\ m^2/s$, 301 lattice nodes were used (corresponding from a dimensional point of view to $\Delta x = 0.003333$ m, and $\Delta t = 1.85 \times 10^{-5} s$). The penalization coefficient was $\eta = 10^{-9}$. To compare the results given by the lattice Boltzmann method applied to the penalized Burgers equation, we also solved the penalized Burgers equation with the finite difference method (where an implicit scheme was employed for the temporal integration, and 301 nodes were also used for the finite difference computations). In Figure 3, where the

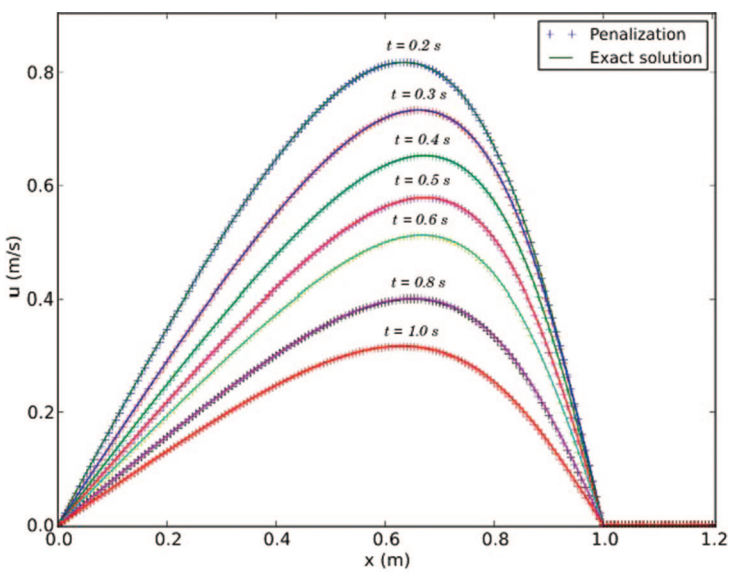

Figure 2: Exact solution (–) and numerical solution (+) (Lattice Boltzmann simulation of the penalized Burgers equation) for a motionless obstacle, at different times

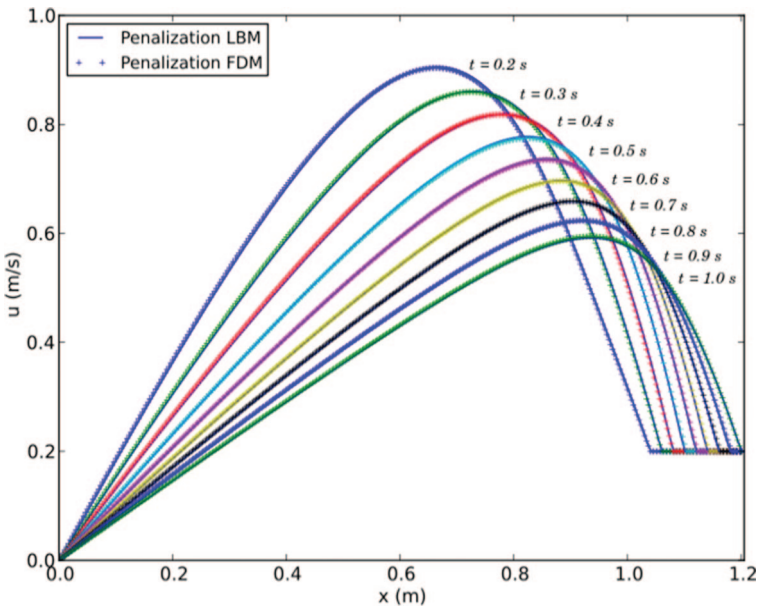

Figure 3: Numerical solutions of Burgers equation, for a moving obstacle with a prescribed motion, at different times. Symbols: – Lattice Boltzmann simulation of the penalized Burgers equation, + solution obtained with a finite difference computation of the penalized Burgers equation

solution at different times is presented, we can see that the interface moves at a constant velocity according to time. We can also notice a good agreement between the numerical results computed with the penalized Burgers equation and the lattice Boltzmann method, and those obtained with the finite difference method.

2.3. COUPLING BETWEEN THE FLUID FORCE CALCULATED WITH THE PENALIZED BURGERS EQUATION AND THE MOTION OF A SOLID OBSTACLE

In this paragraph, we considered that Burgers equation was coupled with the motion of a spring, governed by the following equation:

$$m\ddot{x}_s(t)+k\left(x_s(t)-X_0\right)=F\left(x_s(t)\right) \tag{7}$$

where $x_s(t)$ is the position of the fluid solid interface, m and k are the solid mass and spring constant respectively, X_0 is the spring natural length. $F(x_s(t))$ is the force exerted by the fluid on the obstacle, it was calculated with:

$$F\left(x_s(t)\right)=-\nu\left(\frac{\partial u}{\partial x}\right)_{x_s(t)} \tag{8}$$

The fluid velocity was calculated with the penalized Burgers equation in the lattice Boltzmann framework, in the one dimensional domain $\Omega = [0; 1.2]$. The initial condition was: $u(x, 0) = sin(\pi x), x \in \Omega_f(0) = [0; 1]$, and $u(x, 0) = 0, x \in \Omega_s(0) = [1; 1.2]$. The boundary

condition on the left side of the fluid domain was: $u(0, t) = 0$. The fluid viscosity was: $v = 0.05\ m^2/s$. The parameters relative to the spring were: $X_0 = 0.95$ m, $m = 0.5\ kg$, with two values for the spring constant: k = 39.5 N/m and $k = 0.395\ N/m$. For the lattice Boltzmann simulation, 301 lattice nodes were used (corresponding from a dimensional point of view to $\Delta x = 0.003333$ m, and $\Delta t = 1.85 \times 10^{-5} s$). The penalization coefficient was $\eta = 10^{-9}$. The results obtained with the lattice Boltzmann method are compared with those computed with the finite difference method (with 301 nodes), where the volume penalization method was also applied. In Figure 4, where the position of the interface, according to time, is shown, we can see that, for the case k = 39.5 N/m, the interface displacement was governed by the spring, but it was damped by the fluid forces. For the case $k = 0.395\ N/m$, the force exerted by the spring was small, and the interface motion was mainly due to the fluid forces. In Figure 5, the dimensional velocity profile obtained at time $t = 1\,s$ is also presented.

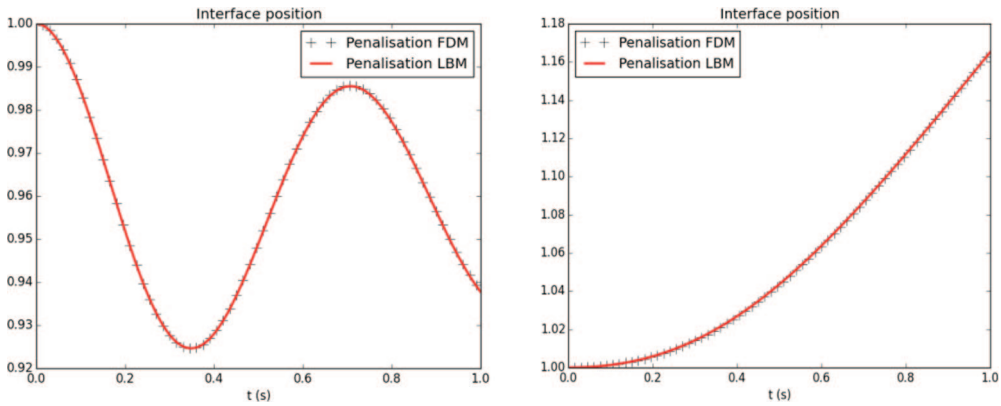

Figure 4: Position of the interface, according to time, for the coupling of Burgers equation with the motion of a spring. Symbols: – Lattice Boltzmann simulation of the penalized Burgers equation, + solution obtained with a finite difference computation of the penalized Burgers equation. a) k = 39.5 N/m, b) k = 0.395 N/m

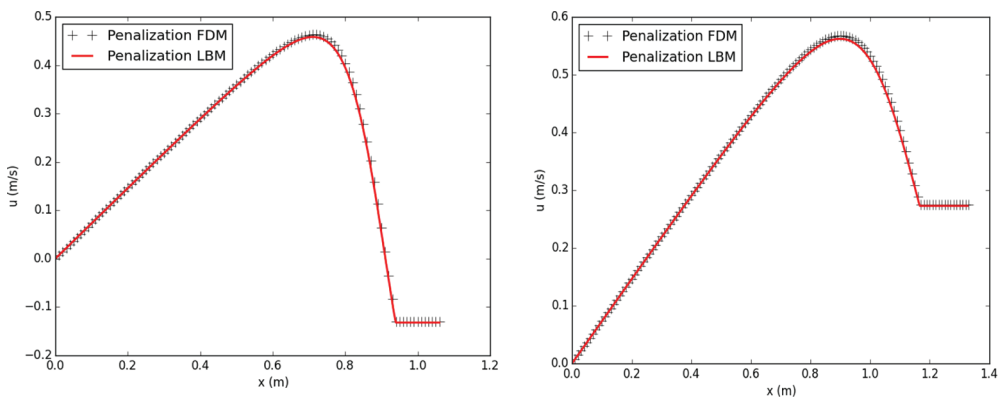

Figure 5: Velocity at $t = 1\ s$, for the coupling of Burgers equation with the motion of a spring. Symbols: – Lattice Boltzmann simulation of the penalized Burgers equation, + solution obtained with a finite difference computation of the penalized Burgers equation. a) k = 39.5 N/m, b) $k = 0.395\ N/m$

In Figures 4 and 5, we can notice that a good adequation was found between the results computed with the volume penalization method applied to the lattice Boltzmann equation, and those obtained with the finite difference method.

3. TWO DIMENSIONAL NAVIER-STOKES EQUATIONS

Next, we applied the volume penalization technique to the Navier-Stokes equations, in the lattice Boltzmann framework. The Navier-Stokes equations where the volume penalization technique was applied, read [19]:

$$\rho\frac{\partial\vec{u}}{\partial t}+\rho\vec{u}\ .\ \nabla\vec{u}=-\nabla p+\mu\nabla\ .\left[\left(\nabla\vec{u}+\left(\nabla\vec{u}\right)^{T}\right)\right]-\frac{\rho}{\eta}\left(\chi\left(\vec{u}-\vec{u}_{s}\right)\right) \tag{9}$$

where μ and ρ are the dynamic viscosity and the density of the fluid considered, $\vec{u}$ is the fluid velocity, and p is the pressure. In this paper where the first step of our work is presented, the Navier-Stokes equations were solved for motionless obstacles $\left(\vec{u}_{s}=\vec{0}\right)$. The continuity equation was satisfied:

$$\nabla\ .\ \vec{u}=0 \tag{10}$$

The lattice Boltzmann method ([22], [23], [24]), which can be easily implemented and is naturally suited for parallel computing, was chosen for solving the flow equations. The lattice Boltzmann equation, with the BGK collision operator, is given in equation 2. Two dimensional flows were computed, and the *D*2*Q*9 lattice model was selected. In the *D*2*Q*9 model, the lattice velocities are $\vec{e}_{0}=(0,0)$, $\vec{e}_{\alpha}=c\left(cos\left((\alpha-1)\pi/2\right),sin\left((\alpha-1)\pi/2\right)\right)$ for α = 1, 2, 3, 4, $\vec{e}_{\alpha}=c\sqrt{2}\left(cos\left((\alpha-5)\pi/2+\pi/4\right),sin\left((\alpha-5)\pi/2+\pi/4\right)\right)$ for α = 5, 6, 7, 8, where $c = \Delta x/\Delta t$. The equilibrium distribution function is:

$$f_{\alpha}^{eq}\left(\vec{x},t\right)=\omega_{\alpha}\rho\left[1+\frac{\vec{e}_{\alpha}\ .\ \vec{u}}{c_{s}^{2}}+\frac{\vec{u}\vec{u}:\left(\vec{e}_{\alpha}\,\vec{e}_{\alpha}-c_{s}^{2}I\right)}{2c_{s}^{4}}\right] \tag{11}$$

where ω_a are the weighting coefficients (for the *D*2Q*9* model: ω_0 = 4/9, ω_α = 1/9 for α = 1, 2, 3, 4, ω_α = 1/36 for α = 5, 6, 7, 8, c_s is the speed of sound ($c_{s}=c/\sqrt{3}$ for the *D*2Q9 model). In the lattice Boltzmann equation (equation 2), the penalization term $\vec{F}=-\frac{\rho}{\eta}\left(\chi\left(\vec{u}-\vec{u}_{s}\right)\right)$ was modelled using the forcing term proposed by Guo et al. ([13]):

$$F_{\alpha}=\left(1-\frac{1}{2\tau}\right)\omega_{\alpha}\left[\frac{\vec{e}_{\alpha}-\vec{u}}{c_{s}^{2}}+\frac{\left(\vec{e}_{\alpha}\ .\ \vec{u}\right)}{c_{s}^{4}}\vec{e}_{\alpha}\right].\vec{F} \tag{12}$$

where the fluid velocity is defined according to:

$$\rho\vec{u}=\sum_{\alpha}\vec{e}_{\alpha}\,f_{\alpha}+\frac{\Delta t}{2}\vec{F} \tag{13}$$

As shown by Guo et al., this model avoids spurious spatial and temporal terms in the continuity and momentum equations. In equation 13, the left hand side and the right hand side are taken at the same time instant. Since the right hand side also contains the fluid velocity (via the penalization term), the fluid velocity was calculated according to the following expression (deduced from equation 13):

$$\vec{u} = \frac{\sum_{\alpha} \vec{e}_{\alpha} f_{\alpha} + \frac{\Delta t}{2} \frac{\chi}{\eta} \rho \vec{u}_s}{\rho + \frac{\Delta t}{2} \frac{\chi}{\eta} \rho} \tag{14}$$

This procedure was applied by Guo and Zhao [25] who built a lattice Boltzmann model in order to compute incompressible flows in porous media, but they did not use the volume penalization technique and treat flows around moving obstacles.

In order to validate the present methodology, two cases were considered: flow past a square obstacle in a channel, and flow past a circular cylinder. For these cases, quantitative results were obtained. The drag force F_d and lift force F_l were computed with the momentum exchange method [1], and the drag and lift coefficients C_d and C_l were deduced:

$$C_d = \frac{F_d}{\frac{1}{2} \rho \, u_{max}^2 D}; \qquad C_l = \frac{F_l}{\frac{1}{2} \rho \, u_{max}^2 D} \tag{15}$$

(where D is a characteristic dimension of the obstacle, and u_{max} is the maximum velocity in a region where the flow is not influenced by the obstacle). The Strouhal number $S_t = \frac{fD}{u_{max}}$ (where f is the frequency of the vortex shedding) was also computed.

3.1. FLOW PAST A SQUARE OBSTACLE

This configuration is depicted in Figure 6. A parabolic velocity profile was applied at the inlet, a zero velocity gradient was applied at the outlet, and no-slip velocity conditions were imposed at the walls. The blockage ratio of this configuration was $B = H/D = 8$, and the length of the channel was $L/D = 50$. In the lattice Boltzmann simulations, the Zou and He ([4]) boundary conditions (i.e. bounce back of the non equilibrium populations) were used. Our results were compared with those obtained by Breuer et al. ([26]) who performed lattice Boltzmann simulations and employed the simple bounce back boundary conditions to impose the no-slip boundary conditions at the walls (walls and square obstacle). Our simulations were conducted with regular grids, and grid refinement tests were done. In this paper, we show the results obtained for ($Re = 20, 40, 100$ $Re = \frac{u_{max} \, D}{\nu}$, where u_{max} is the maximum velocity at the inlet), with the finest grid of 3000 × 480 cells. For this configuration, we carried out simulations using on the one hand the penalization method (with a penalization coefficient of 10^{-9}), and on the other hand the Zou and He bounce back boundary condition at the square obstacle.

In Figure 7, we plotted the streamlines computed with the penalization technique, for $Re = 40$, and $Re = 100$. For low Reynolds numbers, the flow is steady, and two counter-rotating vortices appear symmetrically about the flow axis behind the square obstacle (see

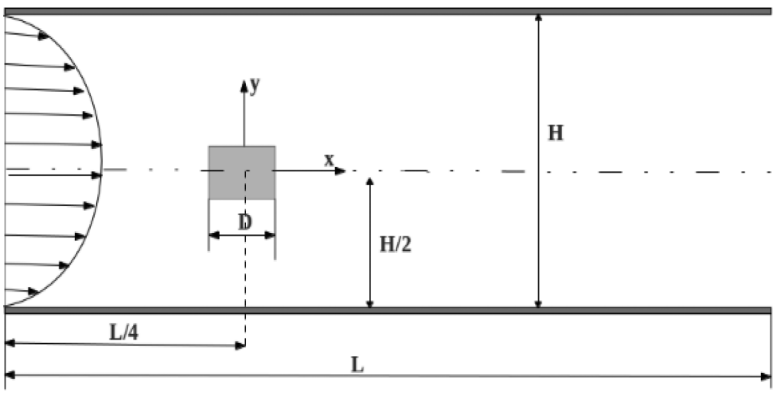

Figure 6: Configuration studied (flow past a square obstacle)

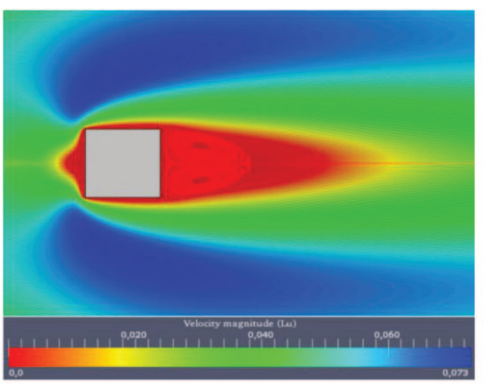

a) $Re = 40$

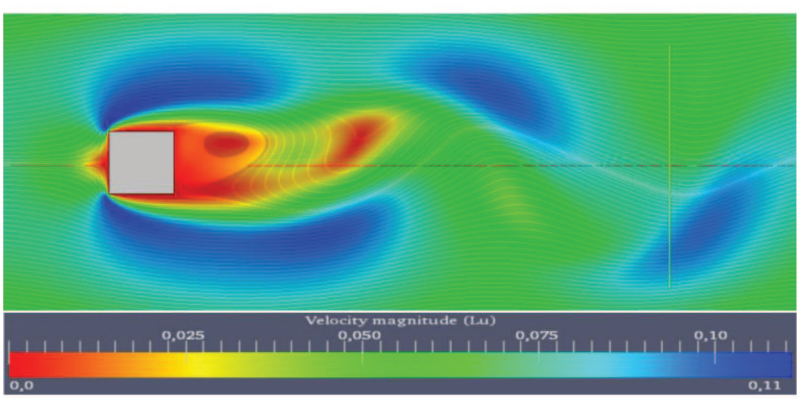

b) $Re = 100$

Figure 7: Streamlines superposed on the velocity magnitude isocontours, flow past a square obstacle computed with the penalization method: a) Re = 40, b) Re = 100

Figure 7a, $Re = 40$). When the Reynolds number is increased, unsteadiness occurs, and a Von Karman vortex street behind the cylinder can be seen as shown in Figure 7b ($Re = 100$).

In Figures 8 and 9, we compare the profiles of streamwise velocity along the flow axis, and the profiles of streamwise velocity in planes perpendicular to the flow axis, computed with the penalization technique, and with the Zou and He bounce back boundary condition,

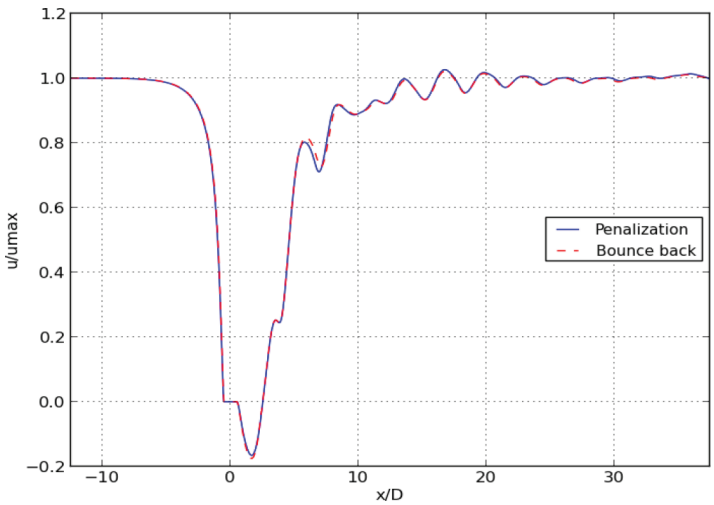

Figure 8: Profiles of streamwise velocity along the flow axis, obtained at $t = 666{,}67s$. ($Re = 100$). Symbols: – penalization technique (LBM framework), –– Zou and He bounce back boundary condition

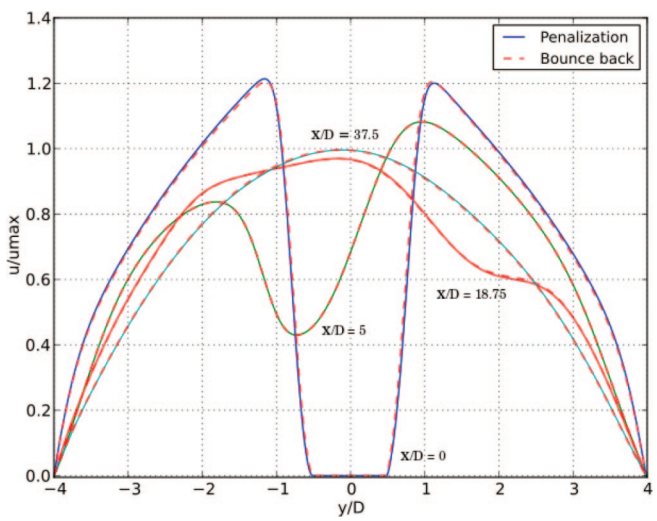

Figure 9: Profiles of streamwise velocity in planes perpendicular to the flow axis, obtained at $t = 666{,}67\,s$. ($Re = 100$). Symbols: – penalization technique (LBM framework), –– Zou and He bounce back boundary condition

for the case Re = 100, at the same time instant (i.e. at 666,67s). We can see that these two techniques yielded similar results.

The non dimensional recirculation length, the drag and lift coefficients, and the Strouhal number were gathered in Table 1, as well as Breuer et al.'s results. We can notice a satisfactory agreement between the results computed with the penalization technique, and those computed with the Zou and He bounce back condition. There is a small discrepancy between our results and Breuer et al.'s results that were obtained on a coarser grid (2000 × 320 cells).

3.2. FLOW PAST A CIRCULAR CYLINDER

The second configuration is shown in Figure 10. The boundary conditions at the horizontal upper and lower planes were symmetry boundary conditions, and a flat velocity profile was applied at the inlet. The boundary condition at the outlet was the same as in the previous case. Three cases were considered: Re = 20, 40 and 100, where the Reynolds number was built using the cylinder diameter, and the constant velocity at the inlet. The domain dimensions were: $L1 = 15\ D$, $L2 = 30\ D$, $H = 60\ D$. Due to the curved geometry of the cylinder, this configuration was more complex than the previous one. A large number of grids were

Table 1: Comparison of recirculation length, drag and lift coefficients, Strouhal number for flow past a square obstacle at Re = 20, 40, 100 ($C_{d\ -\ av}$ is the time-averaged drag coefficient, $(Cl_{max} - Cl_{min})_{av}/2$ is the average of the difference between the maximum and minimum values of the lift coefficient, divided by 2)

Re	Parameter	Penalization	Bounce Back	Breuer et al. [26]
20	L_r/D	1.072	1.044	1.044
	$C_{d\ -\ av}$	2.503	2.479	2.328
	L_r/D	2.221	2.156	2.156
40	$C_{d\ -\ av}$	1.801	1.780	1.717
	$C_{d\ -\ av}$	1.396	1.362	1.378
100	$(Cl_{max} - Cl_{min})_{av}/2$	0.200	0.194	0.182
	S_t	0.138	0.139	0.139

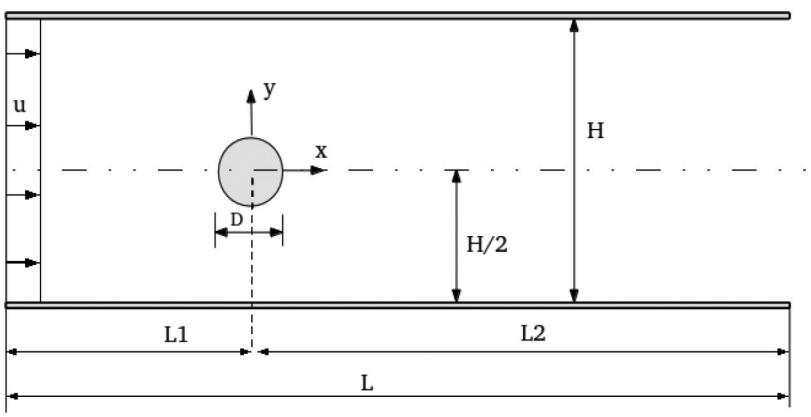

Figure 10: Configuration studied (flow past a circular cylinder)

necessary to compute this flow. A grid independence test was performed for this case; the results presented in this paragraph were computed with the finest grid (1845×2460). For this configuration, the flow around the cylinder was computed with the penalization method on the one hand (with a penalization coefficient of 10^{-9}), and with the bounce back boundary condition proposed by Bouzidi et al. [27] for curved boundaries on the other hand.

The streamlines around the cylinder, computed with the penalization method, are shown in Figure 11. For low Reynolds numbers, symmetric recirculation regions behind the cylinder can be noticed. For higher Reynolds numbers, vortex shedding occurs. With the penalization method, we found that the critical Reynolds number below which the flow is steady was 45. This is in agreement with the critical value of $45 \sim 49$ given in literature.

In Figures 12 and 13 we plotted the profiles of streamwise velocity along the flow axis, and in planes perpendicular to the flow axis, obtained at the same time instant (i.e. at $t = 428{,}32s$). A good agreement between the results computed with the penalized Navier-Stokes equations solved with the lattice Boltzmann method, and those obtained with the bounce back boundary condition applied on the fluid/solid interface of the cylinder, can be highlighted.

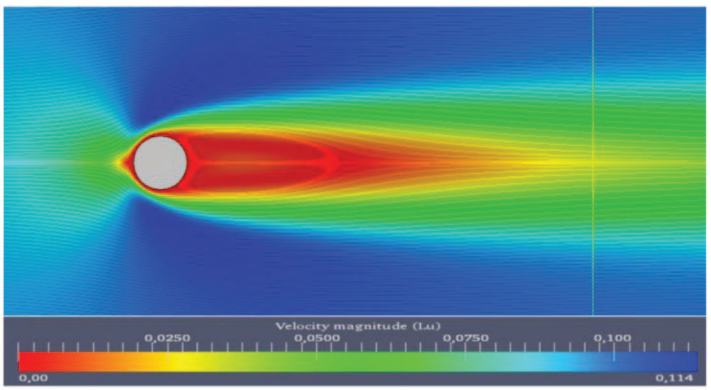

a) $Re = 40$

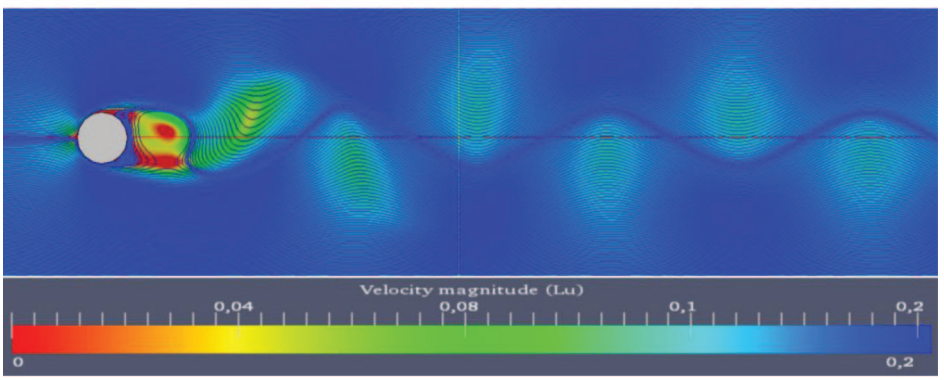

b) $Re = 100$

Figure 11: Streamlines superposed on the velocity magnitude isocontours, flow past a circular cylinder computed with the penalization method: a) $Re = 40$, b) $Re = 100$

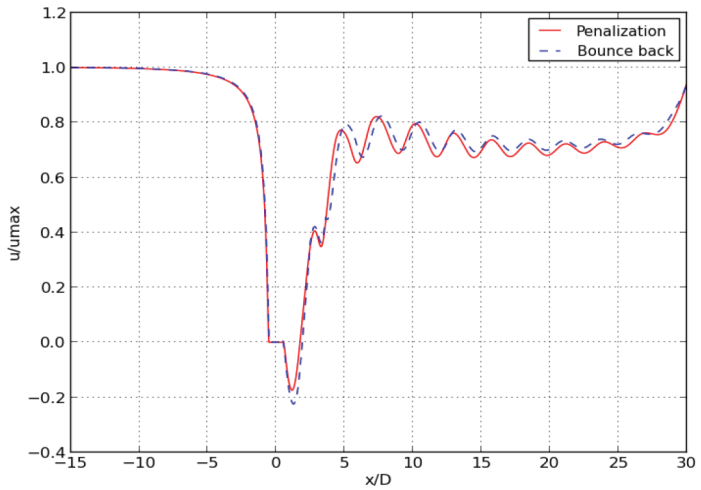

Figure 12: Profiles of streamwise velocity along the flow axis, obtained at $t = 428{,}32s$. ($Re = 100$). Symbols: – penalization technique (LBM framework), –– bounce back boundary condition

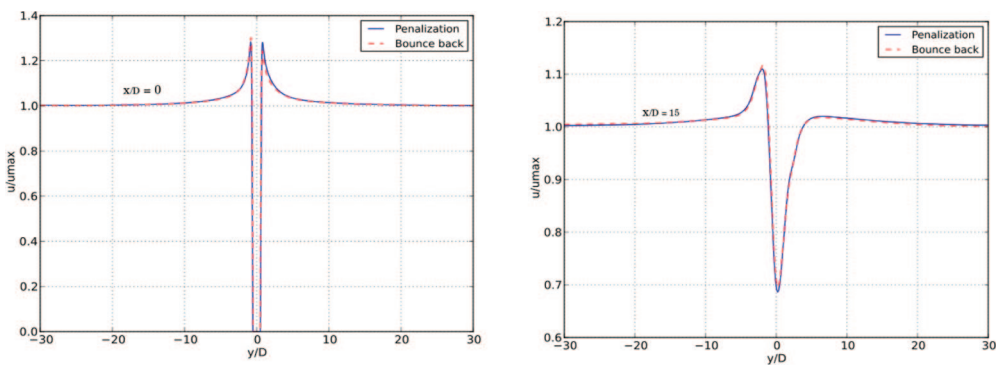

Figure 13: Profiles of streamwise velocity in planes perpendicular to the flow axis, obtained at $t = 428{,}32s$. ($Re = 100$). Symbols: – penalization technique (LBM framework), –– bounce back boundary condition. a) $x/D = 0$, b) $x/D = 15$

The non dimensional recirculation length, the drag and lift coefficients, and the Strouhal number that we computed with the penalization approach, and the bounce back method, are reported in Table 2. In this table, the simulation results of Zhou et al. [28], He and Doolen [29], Wu and Shu [12], and the experimental results of Tritton [30], and Williamson [31] are included for comparison. The simulation results, found in literature, included in Table 2, were obtained by the lattice Boltzmann method, and the non-equilibrium extrapolation method developed by Guo et al [32] (cf Zhou et al.), an interpolation approach applied to a curvilinear grid (cf He and Doolen), an immersed boundary technique (cf Wu and Shu). Although the results computed with the penalization approach were in agreement with the results in literature, we noticed a slightly higher discrepancy for this more complex geometry than for the square obstacle, which may be due to the high number of grids that is necessary when the penalization technique is applied.

Table 2: Comparison of recirculation length, drag and lift coefficients, Strouhal number for flow past a circular cylinder at Re = 20, 40, 100 ($C_{d\ -\ av}$ is the time-averaged drag coefficient, $(Cl_{max} - Cl_{min})_{av}/2$ is the average of the difference between the maximum and minimum values of the lift coefficient, divided by 2)

Re	**Parameter**	**Penalization**	**Bounce Back**	**Zhou et al [28]**
20	L_r/D	1.02	0.92	0.92
	$C_{d\ -\ av}$	2.10	2.07	2.30
Re	**Parameter**	**He and Doolen [29]**	**Wu and Shu [12]**	**Tritton [30]**
20	L_r/D	0.92	0.93	–
	$C_{d\ -\ av}$	2.15	2.09	2.22
Re	**Parameter**	**Penalization**	**Bounce Back**	**Zhou et al [28]**
40	L_r/D	2.36	2.32	2.20
	$C_{d\ -\ av}$	1.59	1.56	1.70
Re	**Parameter**	**He and Doolen [29]**	**Wu and Shu [12]**	**Tritton [30]**
40	L_r/D	2.25	2.31	–
	$C_{d\ -\ av}$	1.50	1.57	1.48
Re	**Parameter**	**Penalization**	**Bounce Back**	**Zhou et al [28]**
	$C_{d\ -\ av}$	1.440	1.407	1.428
100	$(Cl_{max} - Cl_{min})_{av}/2$	0.380	0.369	0.315
	S_t	0.165	0.168	0.172
Re	**Parameter**	**Wu and Shu [12]**	**Williamson [31]**	
	$C_{d\ -\ av}$	1.364	–	
100	$(Cl_{max} - Cl_{min})_{av}/2$	0.344	–	
	S_t	0.163	0.166	

4. CONCLUDING REMARKS AND FUTURE WORK

In this work, a volume penalization technique was employed to simulate flow past obstacles, using the lattice Boltzmann approach. This technique was applied in a first step to the one dimensional Burgers equation. We compared our results for cases of a motionless obstacle, of the forced motion of an obstacle, and of the coupling between the fluid force calculated with the penalized Burgers equation, and the motion of a solid obstacle, with analytical results, and results obtained with the finite difference method, and we noticed a satisfactory accuracy of these results. The second step of our study focused on the numerical prediction of incompressible flows around motionless obstacles (the Navier-Stokes equations). A satisfactory agreement with results found in literature (lattice Boltzmann results and experimental results) was observed. Regular grids were used, and many cells were necessary to obtain grid independent results. A local grid refinement technique is now introduced into our lattice Boltzmann code, in order to decrease the number of cells, and thus the computing time. This will then enable us to treat more easily flows around moving obstacles.

REFERENCES

[1] Anthony J. C. Ladd. Numerical simulations of particulate suspensions via a discretized Boltzmann equation. Part 1. Theoretical foundation. *Journal of Fluid Mechanics, 271:285–309, July 1994*.

[2] Anthony J. C. Ladd. Numerical simulations of particulate suspensions via a discretized Boltzmann equation. Part 2. Numerical results. *Journal of Fluid Mechanics, 271: 311–339, July 1994*.

[3] D.R. Noble and J.R. Torczynski. A lattice-boltzmann method for partially saturated computational cells. *International Journal of Modern Physics C, 9(8):1189–1201, 1998*.

[4] Qisu Zou and Xiaoyi He. On pressure and velocity boundary conditions for the lattice Boltzmann BGK model. *Physics of Fluids (1994-present), 9(6):1591–1598, June 1997*.

[5] Charles S Peskin. Numerical analysis of blood flow in the heart. *Journal of Computational Physics, 25(3):220–252, November 1977*.

[6] Z.G. Feng and E.E. Michaelides. The immersed boundary lattice boltzmann method for solving fluid-particles interaction problems. *J. Comput. Phys., 195:602–628, 2004*.

[7] Ten Cate, A. Nieuwstad, C., Derksen, J. and Van den Akker, H. Particle imaging velocimetry experiments and lattice-Boltzmann simulations on a single sphere settling under gravity. *Phys. Fluids., 14, 11. (2002), 4012–4025*.

[8] Goldstein, D. and Handler, R. and Sirovich, L. Modeling a no-slip flow boundary with external force field. *J. Comput. Phys. 105(1993), 354–366*.

[9] Zhi-Gang Feng and Efstathios E. Michaelides. Proteus: a direct forcing method in the simulations of particulate flows. *Journal of Computational Physics, 202(1):20–51, January 2005*.

[10] Alexandre Dupuis, Philippe Chatelain, and Petros Koumoutsakos. An immersed boundary lattice Boltzmann method for the simulation of the flow past an impulsively started cylinder. *Journal of Computational Physics, 227(9):4486–4498, April 2008*.

[11] E. A. Fadlun, R. Verzicco, Y. P. Orl and J. Mohd-yusof. Combined immersed boundary finitedifference methods for three-dimensional complex flow simulations. *Journal of Computational Physics, pages 35–60, 2000*.

[12] J. Wu and C. Shu. Implicit velocity correction-based immersed boundary-lattice Boltzmann method and its applications. *Journal of Computational Physics, 228(6):1963–1979, April 2009*.

[13] Zhaoli Guo, Chuguang Zheng and Baochang Shi. Discrete lattice effects on the forcing term in the lattice boltzmann method. Physical Review E, 65(4):1–6, April 2002.

[14] R. Glowinski, T. W. Pan, T. I. Hesla and D. D. Joseph. A distributed Lagrange multiplier/fictitious domain method for particulate flows. *International Journal of Multiphase Flow, 25(5):755–794, August 1999*.

[15] Xing Shi and Nhan Phan-Thien. Distributed Lagrange multiplier/fictitious domain method in the framework of lattice Boltzmann method for fluid–structure interactions. *Journal of Computational Physics, 206(1):81–94, June 2005*.

[16] Zhaosheng Yu. A DLM/FD method for fluid/flexible-body interactions. *Journal of Computational Physics, 207(1):1–27, July 2005*.

[17] M. Meldi, E. Vergnault and P. Sagaut. An arbitrary Lagrangian–Eulerian approach for the simulation of immersed moving solids with Lattice Boltzmann Method. *Journal of Computational Physics, 235:182–198, February 2013*.

[18] Jean Donea, Antonio Huerta, J.-Ph. Ponthot and A. Rodríguez-Ferran. Arbitrary Lagrangian–Eulerian Methods. *In Encyclopedia of Computational Mechanics. John Wiley & Sons, Ltd, 2004*.

[19] Philippe Angot, Charles-Henri Bruneau and Pierre Fabrie. A penalization method to take into account obstacles in incompressible viscous flows. *Numerische Mathematik, 81(4):497–520, February 1999*.

[20] Benjamin Kadoch, Dmitry Kolomenskiy, Philippe Angot and Kai Schneider. A volume penalization method for incompressible flows and scalar advection–diffusion with moving obstacles. *Journal of Computational Physics, 231(12):4365–4383, June 2012*.

[21] Baochang Shi and Zhaoli Guo. Lattice Boltzmann model for nonlinear convection-diffusion equations. *Phys. Rev. E, 79:016701, Jan 2009*.

[22] Shiyi Chen and Gary D. Doolen. Lattice Boltzmann Method for Fluid Flows. *Annual Review of Fluid Mechanics, 30(1):329–364, 1998*.

[23] Sauro Succi. The lattice Boltzmann equation: for fluid dynamics and beyond. *Oxford university press, 2001*.

[24] Dazhi Yu, Renwei Mei, Li-Shi Luo and Wei Shyy. Viscous flow computations with the method of lattice Boltzmann equation. *Progress in Aerospace Sciences, 39(5):329–367, July 2003*.

[25] Z. Guo and T. S. Zhao. Lattice Boltzmann model for incompressible flows through porous media. *Phys. Rev. E, 66, 2002*.

[26] M. Breuer, J. Bernsdorf, T. Zeiser and F. Durst. Accurate computations of the laminar flow past a square cylinder based on two different methods: lattice-Boltzmann and finite-volume. *International Journal of Heat and Fluid Flow, 21(2):186–196, April 2000*.

[27] M'hamed Bouzidi, Mouaouia Firdaouss and Pierre Lallemand. Momentum transfer of a Boltzmann-lattice fluid with boundaries. *Physics of Fluids (1994-present), 13(11):3452–3459, November 2001*.

[28] Hao Zhou, Guiyuan Mo, Feng Wu, Jiapei Zhao, Miao Rui and Kefa Cen. GPU implementation of lattice boltzmann method for flows with curved boundaries. *Computer Methods in Applied Mechanics and Engineering, 225–228:65–73, June 2012*.

[29] Xiaoyi He and Gary Doolen. Lattice Boltzmann Method on Curvilinear Coordinates System: Flow around a Circular Cylinder. *J. Comput. Phys. 134, 2(1997), 306–315*.

[30] D. J. Tritton. Experiments on the flow past a circular cylinder at low Reynolds numbers. *Journal of Fluid Mechanics, 6(04):547–567, November 1959*.

[31] C. H. K. Williamson. Vortex Dynamics in the Cylinder Wake. *Annual Review of Fluid Mechanics, 28(1):477–539, 1996*.

[32] Guo, Z. and Zheng, C. and Shi, B. An extrapolation method for boundary conditions in lattice Boltzmann method. *Phys Fluids 14, 6(2002), 2007–2010*.